



IJRASET

International Journal For Research in
Applied Science and Engineering Technology



INTERNATIONAL JOURNAL FOR RESEARCH

IN APPLIED SCIENCE & ENGINEERING TECHNOLOGY

Volume: CAAA-2018 **Issue:** conference **Month of publication:** April 2018

DOI:

www.ijraset.com

Call:  08813907089

E-mail ID: ijraset@gmail.com

Mathematical System Model - Tilt Rotor RPAS

K Rajasekar¹, A Vivek Anand², S Gollakota³, V R Ravi Varma⁴, A Jayaprabu⁵, S K Kavin Prabhu⁶

^{1, 2, 3, 4, 5, 6}Department of Aeronautical Engineering, Bannari Amman Institute of Technology (BIT), Sathyamangalam, Tamil Nadu, India.

Abstract: *The theme of our work is to develop a controlled and stable drone remotely piloted aircraft system (RPAS) model based on V-22 Osprey which is the most suitable platform for our design. The primary advantage in using V-22 Osprey as opposed to the F-35 was higher thrust to weight ratio achievable using propellers. The design consists of an Aluminium chassis with wing arms controlled by servo motors allowing for tilt rotor operation. Control simplifications use this wing along with a rear tail-fan (ducted fan) to directly control all three rotational degrees of freedom. Thrust providing components were selected to best satisfy the constraints of cost, weight and power. To facilitate the creation of an appropriate control system using the physical characteristics of the model drone, a suitable mathematical model was created and the controllers were initially Mat lab Simulink. The model drone was attached to a rope to allow the tuning of the control systems while in a tethered and safe configuration. This contributed to our work goals of controlled and stable hover being achieved.*

Keywords: *Drone, Control system, Linearization method, Space controller.*

I. INTRODUCTION

Vertical Take-off and Landing (VTOL) aircraft are able to take-off with the agility of a helicopter while retaining the efficiency and speed of an airplane during conventional flight. The applications of such an aircraft are vast, ranging from civilian transport to aero medical evacuation and troop deployment (Bell Agusta, 2005; Wilkins, 2001). Currently such aircraft have been limited to military and research applications.

The long range and efficiency associated with conventional aircraft means they can cover large distances and can land where conventional aircraft often cannot. In these locations supplies can be deployed or surveillance obtained without the need for a sizeable landing area. Similar benefits exist for scaled model Remote Controlled (RC) VTOL vehicles. Model aircraft enthusiasts are more often forced to fly their fixed wing aircraft in areas containing open and appropriate ground space necessary for take-off and landing.

However, a model RC VTOL aircraft would allow for such launching from a roof top or an inadequate surface for conventional take-off such as the beach. These needs and potential applications provide the motivation for this project, in the anticipation of designing and building a model VTOL aircraft that is able to be controlled remotely and affordable to everyday enthusiast. To be able to design a state space controller for the model aircraft a set of state-space equations are required. These must be formulated from physical laws and simplified to allow for the development of a working linear controller.

A diagram of the axes system used to derive the equations is presented in figure 5.1. It is important to note that this system does not share the complexities of more common aircraft axes systems.

Moments about axes and angular velocities are not given separate labels. The system originates at the centre of mass of the plane with the longitudinal axis(X) running through the fuselage in the direction of the nose of the plane. The lateral axis(Y) is positive out of the left (port) wing of the plane.

The vertical axis (Z) is positive in the upward direction. All forces, displacements and velocities along each of these three body reference axes are positive in the directions indicated. Pitch moments, angles and angular velocities of the aircraft are positive in a nose-up direction. Yaw moments, angles and angular velocities are positive in the nose-left direction. Roll moments, angles and angular velocities are positive for leftwing down rotations. The aim of this paper is to develop a mathematical model for remote control model VTOL aircraft that is a scale model of a real life aircraft. It should feature a control system which allows the aircraft to remain in stable hover without user intervention. By definition, this aircraft must be able to take off vertically and transition into conventional flight and be able to return to hover mode for landing. It is envisaged that a significant market would exist if a VTOL aircraft could be purchased for a price affordable to the average RC enthusiast. It is desired to make such an aircraft available for under \$2000. During development the aircraft will be controlled via a PC, however the final version must be controllable using a standard RC receiver. It is desirable for the model to be intuitive to fly for someone who is used to flying conventional model aircraft. As such when the model is hovering. The control system should be capable of keeping the model stable with minimal user intervention.

II. STATE EQUATIONS

A. Linearization Methods Used

To allow for the implementation of a state space controller a linearized state model is required. This model is derived from the state equations through the linearization of non-linear terms in the equations. The following simplifications are applied in the derivation of the model.

Where θ is small, we assume in $\sin\theta = \theta$ and $\cos\theta = 1$. The lift generated by the Propellers is proportional to angular velocity squared ($\dot{\theta}_i^2$). We assume that lift can be approximated as a linear function of angular velocity when near the angular velocity required for hover.

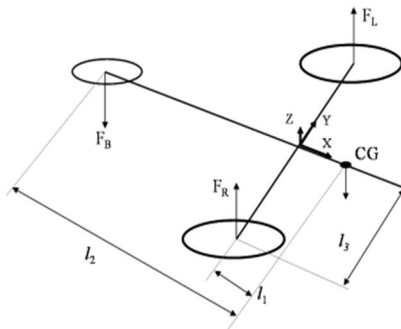


Figure 2.1: Basic Diagram of Model Layout

Hence:

$$\ddot{\theta}_i^2 \approx \dot{\theta}_0 \dot{\theta}_i \tag{2.1}$$

B. Propeller Angles

In order to affect control in various degrees of freedom the propellers are required to rotate independently relative to the XY axis of the plane as in Section 5.2. These angles are θ_L and θ_R (for left and right propeller angles respectively). For transition to normal flight the propellers must both rotate around to the position of a standard plane. However, for the purposes of the state model for hover the rotation angles will be restricted to small values. Gyroscopic affects either directly or indirectly caused by the servo motors or the dynamic movement of angle θ of the propeller are assumed negligible. The servo motors are controlled by Pulse Width Modulation (PWM), so for simplicity it will be assumed that θ is the input to the equations. In practice the Values of θ will be related to the servo motors as PWM outputs from the microcontroller.

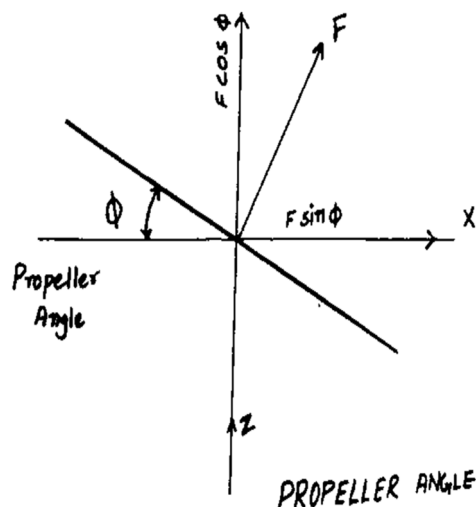


Figure 2.2: Propeller Angles

C. Left and Right Propeller State Equations

The Torque balance and electrical motor equation derivations are directly from the analysis of the Quanser 3DOF Hover platform (Cazzolato, 2005a). If we start with the torque balance from the motor then we have the following non-linear equation:

$$J_m \ddot{\theta}_m + b_m \dot{\theta}_m + k_D (\dot{\theta}_{Mm})^2 = k_T i_a \tag{2.2}$$

Where:

J_m is the moment of inertia of the propeller and motor rotor.

b_m is the viscous friction in the motor rotor.

$k_D (\dot{\theta}_{Mm})^2$ is the reactive torque, in free air, by the propeller due aerodynamic drag.

$k_D > 0$ is the drag constant of the propellers, which is a factor of the air density, the propeller dimensions and other factors.

k_T is the torque constant of the motor.

i_a is the armature current.

θ_m is the angular position of the rotor.

Another system of equations that governs the dynamics IS the electrical equation of the motor:

$$L_a \dot{i}_a + R_a i_a = V_a - k_e \dot{\theta}_m \tag{2.3}$$

where:

L_a is the armature inductance.

R_a is the armature resistance.

k_e is the back EMF constant and is equal to the torque constant of the motor when in SI units.

V_a is the voltage applied to the motor.

In many cases the relative effect Of the Inductance is negligible compared to the mechanical motion and can be neglected In Equation 5.3. This leaves us with:

$$R_a i_a = V_a - k_e \dot{\theta}_m \tag{2.4}$$

Combining equations 5.2 and 5.4 yields:

$$J_m \ddot{\theta}_m + (b_m + \frac{k_T k_e}{R_a} + k_D \dot{\theta}_{m,0}) \dot{\theta}_m = \frac{k_T}{R_a} V_a \tag{2.5}$$

$$J_m \ddot{\theta}_m = \frac{k_T}{R_a} V_a - (b_m + \frac{k_T k_e}{R_a} + k_D \dot{\theta}_{m,0}) \dot{\theta}_m \tag{2.6}$$

Equation 2.6 can be written for each propeller:

$$\ddot{\theta}_L = \frac{1}{J_{prop}} \left(\frac{k_T}{R_a} V_L - K_{mp} \dot{\theta}_m \right) \tag{5.7}$$

$$\ddot{\theta}_R = \frac{1}{J_{prop}} \left(\frac{k_T}{R_a} V_R - K_{mp} \dot{\theta}_m \right) \tag{5.8}$$

Where,

$$K_{mp} = b_m + \frac{k_T k_e}{R_a} + k_D \dot{\theta}_{m,0} \tag{2.9}$$

D. Rear Impeller Equation

The rear ducted fan impeller is expected to have a moment of inertia (J) low enough such that it can be assumed to have negligible effect on the angular acceleration of the impeller. Removing this term from Equation 9 and rearranging yields

$$V_B = \frac{R_B}{k_B} (b_B + \frac{k_B k_e}{R_B} + k_{D, rear} \dot{\theta}_{B,0}) \dot{\theta}_B \quad (2.10)$$

Where:

$$K_B = \frac{R_B}{k_B} (b_B + \frac{k_B k_e}{R_B} + k_{D, rear} \dot{\theta}_{B,0}) \quad (5.9)$$

(2.11)

(5.10)

E. Pitch Axis

Taking the torque balance about the pitch axis, the following expression can be derived:

$$J_p \ddot{p} \approx l_1 (F_L + F_R) - l_2 F_b \quad (2.12)$$

Therefore:

$$\ddot{p} = \frac{l_1}{J_p} (F_L \cos \phi_L + F_R \cos \phi_R) - \frac{l_2}{J_p} F_B \quad (2.13)$$

Simplifying by applying trigonometric linearization:

$$V_B = K_B \dot{\theta}_B \quad \ddot{p} = \frac{l_1}{J_p} (F_L + F_R) - \frac{l_2}{J_p} F_B \approx \frac{l_1 K_{prop}}{J_p} (V_L + V_R) - \frac{l_2 K_{rear}}{J_p} V_B \quad (2.14)$$

Where:

J_p is the moment of inertia of the body about the pitch axis.

l_1 is the distance from the pitch axis to either front propeller centre

l_2 is the distance from the pitch axis to the back propeller centre.

k_1 is the coefficient of lift for the two front propellers.

$K_{1, rear}$ is the coefficient of lift for the back propeller.

It should be noted that the longitudinal distance between the center of mass and the lift point of the propellers (II) is affected by the angle of the motors. The lift point is moved when the motors are not parallel to the pitch axis. This change in l_1 is non-linear and assumed negligible.

F. Roll Axis

Taking the torque balance about the roll axis, the following expressions can be derived:

Therefore:

$$\ddot{r} = \frac{l_3}{J_r} (F_L \cos \phi_L - F_B \cos \phi_R) \quad (2.15)$$

Simplifying by applying trigonometric linearization:

$$\ddot{r} = \frac{l_3}{J_r} (F_L - F_R) = \frac{l_3 K_{prop}}{J_r} (V_L - V_R) \quad (2.16)$$

where:

J_r is the moment of inertia of the body about the roll axis.

l_3 is the distance from the roll axis to either propeller centre.

G. Yaw Axis

Taking the torque balance about the yaw axis yields:

$$J_y \ddot{\gamma} \approx l_3(F_{L,yaw} + F_{R,yaw}) + \tau_L - \tau_R + \tau_B \tag{2.17}$$

$$\ddot{\gamma} = \frac{l_3}{J_y}(F_L \sin \phi_L - F_R \sin \phi_R) + \frac{K_{D,prop}}{J_y}(V_L - V_R) + \frac{K_{D,rear}}{J_y}V_B \tag{2.18}$$

(2.19)

$$\ddot{\gamma} = \frac{1}{J_y}(l_3(F_L \phi_L + F_R \phi_R) + K_{D,prop}(V_L - V_R) + K_{D,rear}V_B)$$

Simplifying by applying trigonometric linearization:

This can be approximated by:

(2.20)

$$\ddot{\gamma} = \frac{1}{J_y}(l_3 K_{prop}(V_L \phi_L + V_R \phi_R) + K_{D,prop}(V_L - V_R) + K_{D,rear}V_B)$$

voltage and propeller angle.

This is linearized by removal of the multiplication between the input

$$\ddot{\gamma} = \frac{1}{J_y}(l_3 K_{prop}(V_{hov} \phi_L + V_{hov} \phi_R) + K_{D,prop}(V_L - V_R) + K_{D,rear}V_B) \tag{2.21}$$

Where:

J_y is the moment of inertia of the body about the yaw axis

l_3 is the distance from the roll axis to either propeller centre.

V_{hov} is the voltage supplied to the front propellers for hover.

H. Vertical Translation

For z-axis translation, it is assumed that in-ground effects are negligible and that the translational velocity is too low to induce significant drag. All translations are expressed in body reference frame.

Therefore:

$$M_P \ddot{z} = \sum F_z \approx F_L \cos \phi_L + F_R \cos \phi_R + F_B - W \tag{2.22}$$

Where $W=Mpg$ the total weight of the model.

Linearizing the cosine terms and replacing the forces with voltage input relationships gives:

$$M_P \ddot{z} = K_{prop}V_L + K_{prop}V_R + K_{rear}V_B - W \tag{2.23}$$

$$M_P \ddot{z} = K_{prop}(V_L + V_R) + K_{rear}V_B - W \tag{2.24}$$

I. Lateral and Longitudinal Translation

For both lateral and longitudinal translation it is assumed that drag is negligible due to low viscosity. Since there is no translation forces acting along the lateral translation is not considered. Thus:

$$M_P \ddot{y} = 0 \tag{2.25}$$

In the longitudinal direction the only translational forces are from the tilted propellers. Thus:

$$M_P \ddot{x} = \sum F_x \approx F_L \sin \phi_L + F_R \sin \phi_R \quad (2.26)$$

Simplifying by applying trigonometric linearization:

$$M_P \ddot{z} = K_{prop}(V_L + V_R) + K_{rear}V_B - W \quad (2.27)$$

This equation can be simplified further by assuming that the motors will be running at a voltage near their hover voltage.

$$M_P \ddot{x} = K_{prop}(V_{hov}\phi_L + V_{hov}\phi_R) \quad (2.28)$$

III. TESTING AND TUNING

A. Initial Open Loop Testing

The group initially tested the model connected rigidly to a rope. This allowed the group to verify the mechanical and systems design. It revealed the flaw in the integrity of the wing arm/motor mount junction. The weight distribution of the model was not proper and hence a fluctuation in the center of gravity was observed under high speed.

B. Closed Loop Testing

It was initially planned to tune the controller while the aircraft was fixed to the rope. This would allow testing with a reduced risk of damage to components (particularly the propellers) from a rough landing, as the consequences of the system going unstable would be minimal. The aircraft was able to be controlled very effectively in the yaw axis through simple proportional feedback. The rope was then loosened to allow the model to attempt a more realistic hover. The roll and pitch axes could not be easily controlled. The layout of the fuselage had been designed for a centre of gravity in front of the lift point of the wings. Moving the pivot point away from this location rendered pitch uncontrollable, with roll dynamics also made uncontrollable as a result.

C. Untethered Testing

The model was tested on the ground outside the Aeronautical department of the Bannari Amman Institute of Technology. This test was short lived as one of the servos hit the ground which caused minor damage to its gear. It was expected that the pitch PID loop would compensate for the pitching forward motion associated with the thrust from the front propellers. However, this proved untrue and a small amount of forwards pitch immediately after takeoff caused the plane to land in such a way that the servo into contact with the ground. The next testing session took place on grass, with the aim of limiting hardware damage due to unstable landings. The power to the tail fan was made proportional to the power supplied to the front motors such that the plane would be more stable in pitch during hover. The maximum power offset “as limited to the point required for stable pitch, in the hope that the pitch PID loop would compensate after this level is reached. The basic PID controller was tested before attempting the more complicated state space controller. The controller gains for roll and pitch were tuned incrementally after each test run. While lift-off was achieved a number of times, the aircraft could not achieve a stable hover. After a few runs the lift-off characteristics were improving with less severe landings. The group did not have time to adequately tune the controller due to a mechanical failure. From its original position and struck the ground. This failure was caused by the plastic servo motor horns stripping and resulted in one of the propellers striking the ground whilst still being powered. However further testing in as not possible due to time constraints.

IV. CONSTRAINT ANALYSIS

A. Cost

Final product price is a major constraint, as a model that is too expensive will have reduced commercial appeal. A project such as this requires the use of several expensive components, which are outlined in Table. Some of these expensive components, such as the IMU will not be used in the final solution but are required for prototyping.

B. Weight

As with any aircraft weight is a major constraint. VTOL aircraft are particularly sensitive to weight as the power plant must produce enough thrust to overcome this weight. The weight distribution of the project model is shown in Table.

C. Power Budget

The amount of power that the batteries can provide is a constraint. Given the specification of a minimum of 3 minutes flight time it is important that the batteries are able to provide full power to the motors for at least this period. The current prototype contains four separate power circuits. The control circuit contains all of the control components and is powered by an 11.1V 1800 mAh LiPo. Each of the main motors is driven by two 1100mAh 11.1V LiPo batteries.

Table 4.1: power, weight and cost budget (HOBBYKING)

S.NO	COMPONENTS	QUANTITY	AMOUNT(Rs.)	COMMENTS	WEIGHT (grams)
1	Motor prop combo - Variable pitch prop & motor set 10" Type A Mounting	2	1463.69*2 =2927.28	Propulsion System	400
2	Servo Motors (small) - Turnigy TGY-50090M Metal Gear 9g Analog Servo	5	265.59*5 = 1327.95	For control surfaces	50
3	Servo Motors (Large) - Turnigy TGY - S901D Metal Gear Digital Robot Servo 13kg/ 0.14sec/ 58g	2	531.72*2 =1063.44	For tilt mechanism	80
4	Electronic Speed Controller - Turnigy Multistar 45 Amp Multi- motor Brushless ESC 2-6S	2	980.40*2 =1960.80	For RPM control of electric motors	30
5	ESC programming card - Turnigy Multistar ESC card	1	216.09	For programming ESC	-
6	Stability Board – MultiWii PRO Flight Controller	1	3473.46	For stabilizing the model	10
7	Battery – Turnigy 5000mAh 3S 20C LiPo Pack	2	1236.42*2 =2472.84	Power system	330
8	Transmitter – Turnigy 9X 9Ch Transmitter w/ Module & 8ch Receiver (Mode 1) (v2 Firmware)	1	2874.15	For signal transmission	-
9	Miscellaneous (Balsa and Frame)	-	5000	Balsa wood and internal frame construction	-
TOTAL			21316.01		900

There were a number of issues relating to the IMU. One issue relating to the IMU that affected several groups, including Jarrett et al. (2004) was the poor handling of two's-complement numbers by Matlab and Simulink and the other was the cost involved in the basic kit of IMU.

V. DISCUSSION AND FUTURE WORK

Whilst a stable hover was not achieved during the course of the project, there were still a number of significant achievements throughout the project.

A. Choice of platform

The first major task in this project was the choice of which platform to base our design on. A number of sources were discussed in the literature review and the reasons against choosing the F-35 Joint Strike Fighter were detailed in Section 3.1. For the reasons outlined in Section 2.2.2, the V-22 Osprey was noted to have some promising features and subsequently was analyzed in more detail. This change in platform necessitated the abandoning of much of the work achieved by Jarrett et al. (2004).

B. Mechanical design

To develop a realistic working model of the system, a full solid model of the frame and components was constructed in CATIA. The biggest constraint was keeping the weight down enough to ensure that the thrust to weight ratio exceeded the chosen minimum of 1.5:1.

C. Component Selection and Procurement

Through the review of the mechanical system requirements as discussed in Section 4.3, the components required to produce thrust, namely the batteries, motors and propellers, were chosen and subsequently purchased. These components, whilst expensive, have enormous potential for producing thrust. Furthermore these components have a high degree of reusability due to their quality, and thus will be used in future projects.

D. Mechanical Construction

The frame design was manufactured in the workshop and was assembled with all the chosen components. The frame displayed a high degree of robustness and controllability, provided the control system was sufficiently tuned. As such makes a solid control platform for future development.

E. Mathematical Modelling

This project intended to implement a state space controller which required an accurate model of the system dynamics. In Chapter 5 the mathematical model of the aircraft whilst in hover was derived using force and moment balancing, motor/propeller response properties and differential equations of motion. In order to design a controller the nonlinear terms were approximated as linear about their operation points.

F. Future Tasks

1) *Stable Hover:* Given the large amount of work that has gone into this project it is envisioned that the completion of all the project goals will only require minimal work. As such all of the Project members have expressed an interest in continuing the project past the official completion date in order to get the aircraft to hover in a stable manner. Through the modification of the gimbal to eliminate the issue of the unmodelled dynamics discussed in Section 10.6, it is expected that a suitable controller could be quickly developed. The aircraft would then be tested.

VI. CONCLUSION

While the mathematical model developed in Chapter 5 is quite detailed, many approximations were required to linearize the model. Due to these approximations some states of the model may be uncontrollable in practice. Different methods of linearizing the equations exist but may have similar issues. Should this be the case with the model presented in Chapter 5, the Matlab System Identification toolkit facilitates the evaluation of linear models of dynamic systems from input-output data. Designing the controller using such a numerical system model is potentially more accurate. This will allow a wider choice of control system as some techniques require an accurate model.

REFERENCES

- [1] Airfield Models (2005). http://www.airfieldmodels.com/information_source/model_aircraft_engines/propellers.html.
- [2] Bell Agusta (2005). http://www.bellaugusta.com/pdf/ba609_2004.pdf.
- [3] Boeing (2005). <http://www.boeing.com/rotorcraft/military/v22>.
- [4] Cazzolato, B. (2005a). 3 Degree of Freedom Hover Tutorial. The University of Adelaide.
- [5] Cazzolato, B. (2005b). Advanced Automatic Control Lecture Notes. The University of Adelaide, Adelaide.
- [6] Cazzolato, B. (2005c). Automatic Control II Lecture Notes. The University of Adelaide, Adelaide.
- [7] Chapman, L. (2005). <http://www.geocities.com/v22chap>.
- [8] Dorf, R. and Bishop, R. (2001). Modern Control Systems. Prentice Hall, New Jersey, 9th edition.
- [9] Franklin, J. A. (2002). Dynamics, Control and Flying Qualities of V/STOL Aircraft.
- [10] Hamel, R. L. R. O. J., Tarek; Mahony (2002). Dynamic modelling and configuration stabilization for an x4-flyer. IFAC 15th Triennial World Congress, Barcelona, Spain.
- [11] Hansen, C. and Snyder, S. D. (1996). Active Control of Noise and Vibration. Spon Press.
- [12] HazelProp (2005). http://www.hartzellprop.com/engineering/engineering_faqs.htm.
- [13] ICARE (2005). Personal correspondence.



10.22214/IJRASET



45.98



IMPACT FACTOR:
7.129



IMPACT FACTOR:
7.429



INTERNATIONAL JOURNAL FOR RESEARCH

IN APPLIED SCIENCE & ENGINEERING TECHNOLOGY

Call : 08813907089  (24*7 Support on Whatsapp)